Chirped-pulse amplification of laser pulses with dispersive mirrors

V. Pervak[1,3]*, I. Ahmad[2,3], S. A. Trushin[2], Zs. Major[1,2], A. Apolonski[1], S. Karsch[1,2], and F. Krausz[1,2]

[1]*Ludwig-Maximilians-Universität München, Am Coulombwall 1, D-85748 Garching, Germany*
[2]*Max-Planck-Institut für Quantenoptik, Hans-Kopfermann-Str. 1, D-85748 Garching, Germany*
[3]*These authors contributed equally to this work.*
[4]*izhar.ahmad@mpq.mpg.de*
**volodymyr.pervak@mpq.mpg.de*

Abstract: We report a novel implementation of chirped-pulse amplification (CPA) by dominantly using dispersive multilayer mirrors for chirp control. Our prototyp dispersive-mirror (DMC) compressor has been designed for a kHz Ti:sapphire amplifier and yielded – in a proof-of-concept study – millijoule-energy, sub-20-fs, 790-nm laser pulses with an overall throughput of ~90% and unprecedented spatio-temporal quality. Dispersive-mirror-based CPA permits a dramatic simplification of high-power lasers and affords promise for their advancement to shorter pulse durations, higher peak powers, and higher average powers with user-friendly systems.

©2009 Optical Society of America

OCIS codes: (320.5520) Pulse compression; (320.7090) Ultrafast lasers; (310.1620) Interference coatings; (310.4165) Multilayer design;

References and links

1. D. Strickland, and G. Mourou, "Compression of amplified chirped optical pulses," Opt. Commun. **56**(3), 219–221 (1985).
2. G. A. Mourou, T. Tajima, and S. V. Bulanov, "Optics in the relativistic regime," Rev. Mod. Phys. **78**(2), 309–371 (2006).
3. M. D. Perry, and G. Mourou, "Terawatt to Petawatt Subpicosecond Lasers," Science **264**(5161), 917–924 (1994).
4. E. Gerstner, "Laser physics: extreme light," Nature **446**(7131), 16–18 (2007).
5. F. Krausz, and M. Ivanov, "Attosecond physics," Rev. Mod. Phys. **81**(1), 163–234 (2009).
6. T. Brabec, and F. Krausz, "Intense few-cycle laser fields: frontiers of nonlinear optics," Rev. Mod. Phys. **72**(2), 545–591 (2000).
7. E. B. Treacy, "Optical pulse compression with diffraction gratings," IEEE J. Quantum Electron. **5**(9), 454–458 (1969).
8. M. Pessot, P. Maine, and G. Mourou, "1000 Times Expansion Compression of Optical Pulses for Chirped Pulse Amplification," Opt. Commun. **62**(6), 419–421 (1987).
9. Z. Cheng, F. Krausz, and C. Spielmann, "Compression of 2 mJ kilohertz laser pulses to 17.5 fs by pairing double-prism compressor: analysis and performance," Opt. Commun. **201**(1-3), 145–155 (2002).
10. G. Pretzler, A. Kasper, and K. J. Witte, "Angular chirp and tilted light pulses in CPA lasers," Appl. Phys. B **70**(1), 1–9 (2000).
11. A. L. Cavalieri, E. Goulielmakis, B. Horvath, W. Helml, M. Schultze, M. Fieß, V. Pervak, L. Veisz, V. S. Yakovlev, M. Uiberacker, A. Apolonski, F. Krausz, and R. Kienberger, "Intense 1.5-cycle near infrared laser waveforms and their use for the generation of ultra-broadband soft-x-ray harmonic continua," N. J. Phys. **9**(7), 242 (2007).
12. F. Tavella, Y. Nomura, L. Veisz, V. Pervak, A. Marcinkevičius, and F. Krausz, "Dispersion management for a sub-10-fs, 10 TW optical parametric chirped-pulse amplifier," Opt. Lett. **32**(15), 2227–2229 (2007).
13. R. Szipocs, K. Ferencz, C. Spielmann, and F. Krausz, "Chirped multilayer coatings for broadband dispersion control in femtosecond lasers," Opt. Lett. **19**(3), 201–203 (1994).
14. F. X. Kärtner, N. Matuschek, T. Schibli, U. Keller, H. A. Haus, C. Heine, R. Morf, V. Scheuer, M. Tilsch, and T. Tschudi, "Design and fabrication of double-chirped mirrors," Opt. Lett. **22**(11), 831–833 (1997).
15. R. Szipöcs, A. Köházi-Kis, S. Lakó, P. Apai, A. P. Kovács, G. Debell, L. Mott, A. W. Louderback, A. V. Tikhonravov, and M. K. Trubetskov, "Negative dispersion mirrors for dispersion control in femtosecond lasers: chirped dielectric mirrors and multi-cavity Gires-Tournois interferometers," Appl. Phys. B **70**, S51–S57 (2000).
16. B. Golubovic, R. R. Austin, M. K. Steiner-Shepard, M. K. Reed, S. A. Diddams, D. J. Jones, and A. G. Van Engen, "Double Gires-Tournois interferometer negative-dispersion mirrors for use in tunable mode-locked lasers," Opt. Lett. **25**(4), 275–277 (2000).

#117886 - $15.00 USD Received 28 Sep 2009; accepted 2 Oct 2009; published 8 Oct 2009
(C) 2009 OSA

17. N. Matuschek, L. Gallmann, D. H. Sutter, G. Steinmeyer, and U. Keller, "Back-side-coated chirped mirrors with ultra-smooth broadband dispersion characteristics," Appl. Phys. B **71**(4), 509–522 (2000).
18. G. Tempea, V. Yakovlev, B. Bacovic, F. Krausz, and K. Ferencz, "Tilted-front-interface chirped mirrors," J. Opt. Soc. Am. B **18**(11), 1747–1750 (2001).
19. P. Baum, M. Breuer, E. Riedle, and G. Steinmeyer, "Brewster-angled chirped mirrors for broadband pulse compression without dispersion oscillations," Opt. Lett. **31**(14), 2220–2222 (2006).
20. V. Pervak, F. Krausz, and A. Apolonski, "Dispersion control over the ultraviolet-visible-near-infrared spectral range with HfO2/SiO2-chirped dielectric multilayers," Opt. Lett. **32**(9), 1183–1185 (2007).
21. V. Pervak, C. Teisset, A. Sugita, S. Naumov, F. Krausz, and A. Apolonski, "High-dispersive mirrors for femtosecond lasers," Opt. Express **16**(14), 10220–10233 (2008).
22. V. Pervak, I. Ahmad, M. K. Trubetskov, A. V. Tikhonravov, and F. Krausz, "Double-angle multilayer mirrors with smooth dispersion characteristics," Opt. Express **17**(10), 7943–7951 (2009).
23. M. K. Trubetskov, A. V. Tikhonravov, and V. Pervak, "Time-domain approach for designing dispersive mirrors based on the needle optimization technique. Theory," Opt. Express **16**(25), 20637–20647 (2008).
24. V. Pervak, A. Tikhonravov, M. Trubetskov, S. Naumov, F. Krausz, and A. Apolonski, "1.5-octave chirped mirror for pulse compression down to sub-3 fs," Appl. Phys. B **87**(1), 5–12 (2007).
25. V. Pervak, I. Ahmad, J. Fulop, M. K. Trubetskov, and A. V. Tikhonravov, "Comparison of dispersive mirrors based on the time-domain and conventional approaches, for sub-5-fs pulses," Opt. Express **17**(4), 2207–2217 (2009).
26. A. V. Tikhonravov, and M. K. Trubetskov, *www.optilayer.com*
27. T. V. Amotchkina, A. V. Tikhonravov, M. K. Trubetskov, D. Grupe, A. Apolonski, and V. Pervak, "Measurement of group delay of dispersive mirrors with white-light interferometer," Appl. Opt. **48**(5), 949–956 (2009).
28. P. Tournois, "Acousto-optic programmable dispersive filter for adaptive compensation of group delay time dispersion in laser systems," Opt. Commun. **140**(4-6), 245–249 (1997).
29. S. Sartania, Z. Cheng, M. Lenzner, G. Tempea, Ch. Spielmann, F. Krausz, and K. Ferencz, "Generation of 0.1-TW 5-fs optical pulses at a 1-kHz repetition rate," Opt. Lett. **22**(20), 1562–1564 (1997).
30. W. Koechner, "Solid State laser engineering, Springer series in Optical Science," Springer-Verlag Berlin Heidelberg, 4th edition, (1996).

1. Introduction

Chirped-pulse amplification (CPA) [1] of ultrashort light pulses in solid-state lasers and parametric amplifiers has permitted the generation of optical pulses with multi-gigawatt to multi-terawatt peak powers and holds promise for scaling high-power laser technology far beyond the petawatt frontier [2–4]. CPA systems are now commonplace in laser laboratories and constitute a pivotal research tool in nonlinear optics, ultrafast spectroscopy [5,6], and high-field science [2]. Chirped-pulse amplifiers are seeded with low-energy ultrashort pulses temporally broadened in a dispersive pulse stretcher to permit for amplification without damaging the gain medium. The chirp of the amplified pulses is subsequently removed in a pulse compressor introducing a group-delay dispersion (GDD) of opposite sign. The pulse duration is thereby restored close to that of the input pulse. Conventional CPA systems rely on rather lossy, complex and alignment-sensitive systems of gratings [7,8] and/or prisms [9] for pulse stretching and recompression, which have compromised the production efficiency and the spatio-temporal quality of the amplified pulses. When diffraction gratings or prisms are used in stretchers/compressors, their angular dispersion introduces the desired wavelength-dependent delay. The alignment sensitivity of these components poses a serious challenge in the day-to-day operation of CPA systems. Minute deviations from optimum prism and grating orientations lead to angular chirp and pulse front tilt. The consequence is the deterioration of the pulse profile in focus, both spatially and temporally [10], which may be additionally impaired by thermal and nonlinear effects in these optical components. Moreover, their relatively large amount of uncompensated higher-order dispersion requires the use of additional dispersion management such as dispersive multilayer mirrors [9,11], or hybrid (prism-grating-material) stretcher-compressor systems [12] for bandwidth-limited pulse generation in broadband (10-fs-scale) amplifiers. Here, we report a novel implementation of CPA that overcomes these problems by using dominantly dispersive multilayer mirrors for chirp control. It is the result of a 15-year evolution of the design and fabrication of dispersive multilayers [13–25], which has now allowed the development of structures with low-loss and high dispersion over a wide spectral range. Our prototypical dispersive-mirror compressor (DMC) has been designed for a kHz Ti:sapphire amplifier and yielded – in a proof-of-concept study – millijoule-energy, sub-20-fs, 790-nm laser pulses with an overall throughput of ~90%

#117886 - $15.00 USD Received 28 Sep 2009; accepted 2 Oct 2009; published 8 Oct 2009
(C) 2009 OSA

and unprecedented spatio-temporal quality. Dispersive-mirror-based CPA permits a dramatic simplification of high-power lasers and affords promise for their advancement to shorter pulse durations, higher peak powers, and higher average powers with user-friendly systems.

Dispersive mirrors offer the potential for eliminating these drawbacks owing to their capability of providing tailored dispersion over unprecedented bandwidths *without* spatial separation of spectral components. The wavelength-dependent delay originates from short propagation through virtually lossless, highly dispersive multilayered media. CPA implemented with dispersive mirrors is therefore intrinsically free from the angular chirp, pulse-front tilt and nonlinear effects with the added benefit of higher-order dispersion control. They can be designed to provide GDD of either sign and hence compensate material dispersion both in the visible/near-infrared and the mid-infrared spectral range, where the dispersion of most materials changes its sign.

The exploitation of this potential calls for multilayer structures with high GDD and low loss (denoted by L) over a spectral range of several tens of THz. The figure of merit $FOM = |GDD|/L$ determines the loss at the expense of which a certain amount of dispersion for a certain stretching factor can be realized. The first generation of chirped multilayer mirrors has typically exhibited a GDD of several tens of fs^2 with a loss of a fraction of a percent [13,20,21]. Stretching the duration of sub-50-fs pulses by a factor of ~10^3 requires a GDD of the order of tens of thousands of fs^2. This demand would have called for a prohibitively large number of bounces leading to excessive overall losses with early-generation chirped multilayers.

Recent progress in the design and manufacture of multilayer high-dispersive mirrors (HDM) [21] has resulted in a quantum leap in enhancing the *FOM*, and opened the door for an all dispersive-mirror compressor (DMC) for CPA.

2. Design and fabrication of high dispersive mirrors

The new approach [15] has overcome the limitations of the conventional chirped-mirror technology by exploiting the so-called penetration and resonance effects simultaneously, combining thereby the advantages of chirped mirrors [13] and Gires-Tournois interferometer structures [9,10], respectively (see Fig. 1 for explanation of these effects). However, the high *FOM* of first-generation HDMs came at the expense of a relatively narrow bandwidth, supporting pulses with a duration of slightly shorter than 100 fs only [21]. Here, we present a new generation of HDMs with $GDD \approx$-500 fs^2 and $L < 0.2\%$ per bounce over a wavelength range as broad as 735–845 nm. In addition, GDD variations are smoothened by the combination of penetration and resonance effects. These mirrors can support sub-20 fs pulses and realize a compression factor of ~500 with a throughput of >90%, which allows – for the first time – for the implementation of CPA without having to rely on spatial (transverse) separation of the different spectral components of the amplified beam.

#117886 - $15.00 USD Received 28 Sep 2009; accepted 2 Oct 2009; published 8 Oct 2009
(C) 2009 OSA

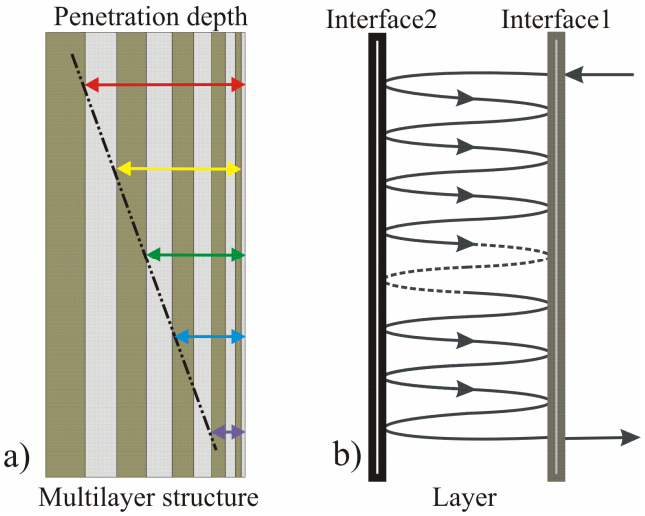

Fig. 1. **GDD via wavelength-dependent penetration (a) and resonant storage (b). (a)** The optical thickness of individual layers changes gradually in a chirped dielectric multilayer structure. This causes wavepackets of different carrier wavelengths to penetrate to a different extent and hence acquire different group delays. In this example, longer wavelengths penetrate deeper, resulting in negative GDD. **(b)** Two interfaces separated by an optical distance corresponding to the half wavelength of the incident radiation resonantly enclose the impinging wave. Such nanoscale Fabry-Perot-interferometers embedded in the multilayer structure can introduce large group delays at selected wavelengths. The new HDMs reported in this work make use of a combination of both effects.

The structure of our multilayer HDM is depicted in Fig. 2(a). It incorporates a large number of layers with slowly varying optical thickness characteristic of a chirped mirror enclosing several Fabry-Perot-like resonant structures. We use tantalum pentoxide (Ta_2O_5) and silicon dioxide (SiO_2) as high and low refractive index materials, i.e. with n = 2.12 and n = 1.47 at 800 nm, respectively. They are considered an optimum choice for high dispersion and low loss in this spectral range [20,21,25]. Figure 2(b) plots the modulus-square of the electric field distribution inside the structure. It reveals that the modulus-square of the electric field in the range of 820-845 nm has the same penetration depth, and the group delay (GD) resulting purely from the penetration effect exhibits strong oscillations between 735 nm and 820 nm as indicated by the yellow contour line. In order to cover the desired spectral range and to minimize spectral variations of the GDD – as a key innovation – we embed a series of resonant cavities in the chirped multilayer structure. They are introduced at locations where the GDD oscillations due to the penetration effect appear, resulting in a highly smoothened GDD curve, as shown by the blue line in Fig. 2(c). Our HDMs are designed to provide 160 fs of GD difference between the edges of the wavelength range of 735–845 nm. Since the maximum delay related to penetration is only 70 fs for a 10-µm thick structure, the combination of penetration and resonance effects allows to enhance the GDD by a factor of ~2.3 without increasing the physical thickness of the entire coating.

#117886 - $15.00 USD Received 28 Sep 2009; accepted 2 Oct 2009; published 8 Oct 2009
(C) 2009 OSA

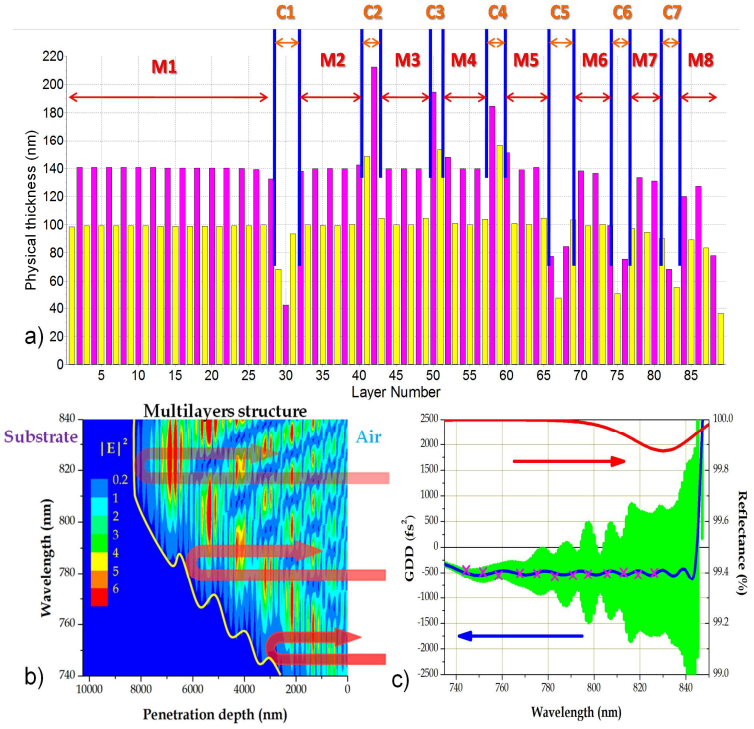

Fig. 2. **Structure and characteristics of our multilayer HDM.** (**a**) Physical thicknesses of the alternate layers of tantalum pentoxide (Ta_2O_5) and silicon dioxide (SiO_2) are shown with yellow and pink columns, respectively. Individual layer thicknesses range between 35 nm and 210 nm and the total physical thickness of the structure is approximately 10 µm. The structure can be represented as a combination of eight mirrors (M1–M8) and seven resonant cavities (C1–C7) resulting in GDD originating from the penetration and resonance effects, respectively. In general the cavities C1–C7 consist of several layers of different materials. (**b**) The distribution of the modulus-square of the electric field ($|E|^2$) displaying the penetration in the HDM structure shown in panel (a). The storage effect of the cavities manifests itself in localized enhancements of the trapped fields. The yellow line plots the GD variation introduced by the penetration effect only. (**c**) Calculated reflectance (red) and GDD (blue) curve of the HDM for the designed angle of incidence of 10°. Measured GDD with white light interferometer (magenta crosses). The green area represents the probable range of GDD values, see text for details.

Successful fabrication of the HDMs can be as challenging as their design. The main problem is connected with the high sensitivity of the GDD curve to even small errors in the layer thicknesses. We scrutinize our HDM design by means of standard computational error analysis. The layer thicknesses of a given design are randomly varied with 1 nm standard deviation. This value corresponds to the accuracy of our state-of-the-art magnetron sputtering machine (Helios, Leybold Optics GmbH, Alzenau, Germany), which is currently one of the most precise devices available for the fabrication of dispersive optics [20–25]. For each perturbed design we computed the GDD and performed a statistical analysis of the obtained GDD dependencies. The GDD design curve of the HDMs, obtained with the Optilayer software [26] for fixed layer thicknesses, is shown in Fig. 2(c) by the blue curve. The green area represents a band obtained after random layer variations that encloses the GDD curve with a probability of 68.3%. As indicated by the magenta crosses, the measured GDD of the HDMs using a white light interferometer [27] shows excellent agreement with the design curve. We confirmed the reliability of our technology with an independent second coating run which delivered similar dispersion characteristics. This analysis reveals that the actual layer-thickness uncertainty of our coating machine is well below the specifications given by the

#117886 - $15.00 USD Received 28 Sep 2009; accepted 2 Oct 2009; published 8 Oct 2009
(C) 2009 OSA

manufacturer, which allows us to fabricate our HDMs in a highly reproducible and reliable way.

3. Compression of pulses with dispersive mirrors

In order to test the performance of our advanced HDMs in a CPA system, we use a commercial multipass Ti:sapphire laser (Femtopower Pro, Femtolasers GmbH). The schematic layout of the experimental setup is shown in Fig. 3. A Ti:sapphire oscillator (Rainbow, Femtolasers GmbH) delivers sub-7 fs seed pulses with few-nJ pulse energy at 70 MHz. They are stretched by 30 mm of SF57-glass and an acousto-optic programmable dispersive filter [28] (DAZZLER, FASTLITE), which provides fine dispersion control, before coupling them into the amplifier. The amplifier is a 10-pass Ti:sapphire based system [29] operating at 1 kHz, pumped at 527 nm by the frequency-doubled output of a Nd:YLF laser (DM30, Photonics Industries). It delivers 1.4 mJ pulses with a FWHM bandwidth of 62 nm centred at 790 nm.

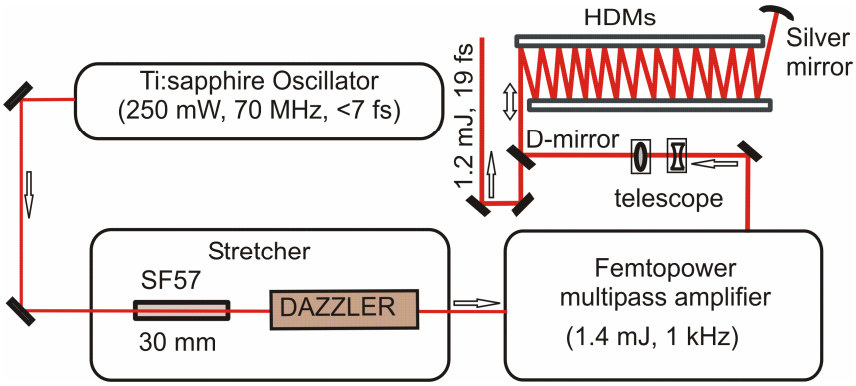

Fig. 3. Schematic layout of the experimental setup. The seed pulses from a Ti:sapphire oscillator are stretched by 30 mm of SF57-glass and an acousto-optic programmable dispersive filter (DAZZLER), which provides fine dispersion control. The amplifier delivers 1.4-mJ pulses at 1 kHz. After amplification, a total of 52 reflections on HDMs are used to compress these pulses down to ~19 fs.

Our dispersion management, for finding the chirp in the amplified pulses and required number of reflections of the HDMs for pulse compression, involves the calculation of the coefficients D_i of the Taylor expansion of the spectral phase $\phi(\omega)$ given by $D_i = \left(\partial^i \phi(\omega) / \partial \omega^i \right)\Big|_{\omega=\omega_0}$. This is accomplished by taking into account the physical thicknesses of all the optical components in the setup. These components are as follows: Faraday rotator (polarizers: 2 × 16 mm calcite; compensator plate: 4 mm quartz; 21 mm TGG), stretcher (30 mm SF57-glass; DAZZLER: 25 mm TeO_2), Ti:sapphire crystal (10 × 4 mm), brewster windows: (20 × 1 mm fused-silica), pulse selector (20 mm DKDP; polarizers: 2 × 11 mm SK10); 3 mm LiNbO3; Berek-compensator: 4 mm MgF_2, windows: 2 × 5 mm fused-silica), lenses (4 × 4 mm BK7), and 15 m of air path. The significance of most of these optical components is described by Sartania et al. [29]. The calculated coefficients of dispersion of the amplified pulses at wavelength $\lambda_0 = 2\pi c/\omega_0 = 790$ nm without any programmed-dispersion from the DAZZLER are $D_2 = +34700$ fs^2 (GDD), $D_3 = +22000$ fs^3 (third-order dispersion) and $D_4 = -7000$ fs^4 (fourth-order dispersion). The DAZZLER is programmed to provide D_2 (or GDD) = -8700 fs^2 and to compensate the higher-order dispersion (D_3 and D_4) of the amplified pulses and that of the HDMs if any. Therefore the pulses leave the amplifier with an overall dispersion of $D_2 = +26000$ fs^2. Since the HDMs are designed to provide -500 fs^2 per reflection, therefore a total of 52 reflections are needed for compression. Fourier transform calculations, by assigning this dispersion to the bandwidth-limited pulse of the amplifier

#117886 - $15.00 USD Received 28 Sep 2009; accepted 2 Oct 2009; published 8 Oct 2009
(C) 2009 OSA

spectrum, predict the stretched pulse duration of ~8.3 ps over the range of 735-845 nm (or 4.8 ps FWHM). This corresponds to an energy-fluence of ~0.6 J/cm^2 under our conditions at 1.4 mJ, which is close to the saturation fluence of 0.9 J/cm^2 and well below the surface damage threshold of 5-10 J/cm^2 for Ti:sapphire crystals [30]. Moreover our calculated B-integral for the last amplifier pass, $B = \frac{2\pi}{n_0 \lambda_0} \int n_2 I(z) dz = 0.6 < 1$, where $n_2 = 3.2 \times 10^{-16}$ cm^2/W for sapphire, $n_0 = 1.76$ at $\lambda_0 = 790$ nm and z = 4 mm, is also within the limits to operate the amplifier safely at 1.4 mJ without any prominent distortion in the spatial and spectral phase of the amplified pulse. Under these conditions the total extraction efficiency is 9.1%.

After amplification, we employ our newly-developed DMC for pulse compression. The beam diameter of its output is magnified to ~7 mm by using a 1:1.5-telescope. A D-cut mirror (D-mirror) is used to couple the beam into the compressor. A total of twenty-six 1″-diameter HDMs separated by 96 mm for an angle of incidence of 10 ± 1° are used in a 2-pass configuration. After the first pass, an f = 3.5 m silver mirror is used to fold the beam path for the second pass and to collimate the beam. It is coupled out by changing the height on the D-mirror in order to keep the angle of incidence identical for both passes. In this configuration, we achieve an overall DMC throughput of 90%.

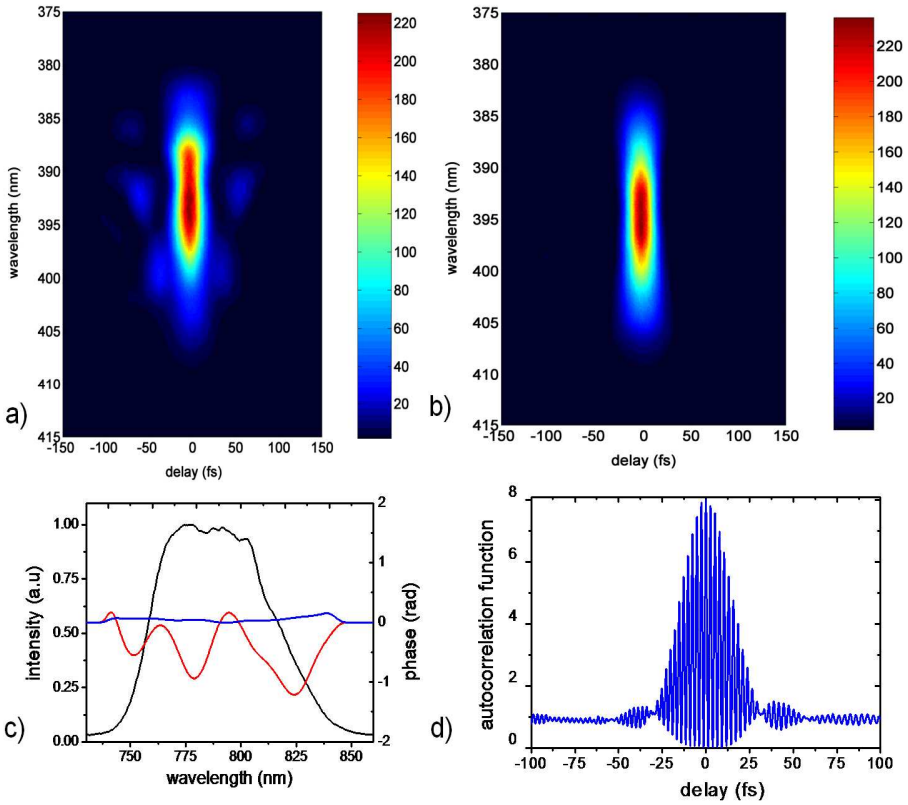

Fig. 4. Temporal characterization of the compressed pulses. Pulse characterization is performed using the GRENOUILLE (Swamp Optics) and 2nd order interferometric autocorrelator (Femtolasers GmbH) devices. (a) The FROG trace without phase file in the DAZZLER, showing satellite pulses due to uncompensated phase oscillations. (b) The FROG trace of the compressed pulses after DAZZLER compensation. (c) The spectrum (black) and the phase of the compressed pulse (blue). The residual phase oscillations after 52 reflections on HDMs (red) before compensation by the DAZZLER (see text). This fine correction reduces the pulse duration by ca. 3 fs. (d) The measured 2nd order interferometric autocorrelation showing 13.8 fringes which corresponds to 19.1 fs assuming a sech-squared temporal shape.

#117886 - $15.00 USD Received 28 Sep 2009; accepted 2 Oct 2009; published 8 Oct 2009
(C) 2009 OSA

The compressed pulses are characterized by frequency-resolved optical-gating (FROG) and second order interferometric autocorrelation. The results of these measurements are summarized in Fig. 4.

Residual GDD oscillations in our DMC imprint a (maximum-to-minimum) spectral phase oscillation of ~1.4 rad on the compressed pulses, as shown by the red curve in Fig. 4(c), which has been retrieved from the FROG trace in Fig. 4(a). Although in principle this could be further optimized by fine-tuning the angle of all 26 HDMs, in our experiment these oscillations were largely removed by the DAZZLER. Since the introduced corrections are small, this did not compromise its throughput. The result is a nearly flat spectral phase (blue curve in Fig. 4(c), retrieved from Fig. 4(b)) and a near Fourier-limited compressed pulse with a duration of 19.1 fs (FWHM), see Fig. 4(d). This value only differs by 0.5% from the calculated transform limited pulse duration of 19 fs for the experimentally determined spectrum.

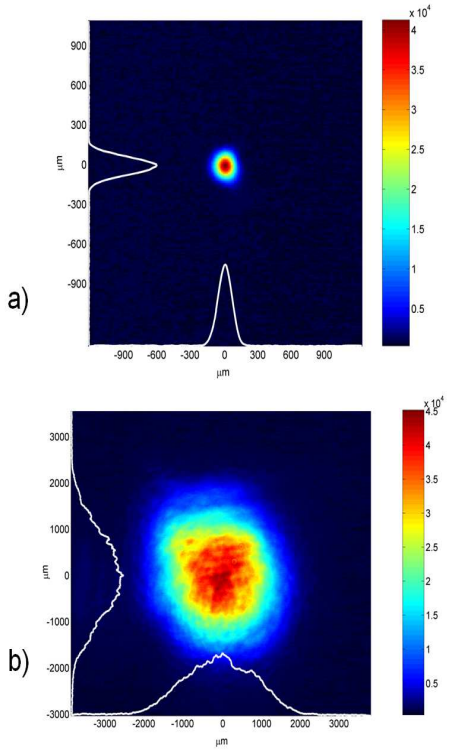

Fig. 5. **Beam profile of pulses compressed with the DCM**. (**a**) The beam profile in the far-field of a 1.5 m focal length lens showing an excellent beam quality with >96% ellipticity for a $1/e^2$ spot size of 250 μm. (**b**) The near-field beam profile with >85% ellipicity for a $1/e^2$ spot size of 3.5 mm.

The spatial characterization of the amplified and compressed pulses yield nearly ideal Gaussian beam profiles both in the near and the far fields (see Fig. 5), demonstrating the capability of the DMC to transmit the compressed femtosecond beam without a distortion of its spatial properties.

4. Conclusion

We have demonstrated that newly-developed low-loss broadband high-dispersion mirrors are capable of taking over the role of prisms and gratings in femtosecond chirped-pulse amplifiers. Our HDMs reach the maximum spectral bandwidth that can be achieved in currently available solid-state CPA systems, introducing a GDD of -500 fs^2 at the expense of less than 0.2% loss per reflection. An all dispersive-mirror compressor, being intrinsically free

#117886 - $15.00 USD Received 28 Sep 2009; accepted 2 Oct 2009; published 8 Oct 2009
(C) 2009 OSA

from nonlinear effects, spatial and angular chirps, eradicates all main hurdles of CPA-systems in reaching near bandwidth-limited compressed pulses with excellent spatial quality. It provides remarkable simplifications in dispersion management. This development opens the way towards simple, alignment insensitive, compact and user-friendly sub-terawatt-scale prism/grating-free kilohertz femtosecond laser systems. The performance of the prototypical HDMs used in this proof-of-principle study may be far from what will be ultimately feasible. Substantial enhancement of the figure of merit of HDMs may permit the advancement of DMC technology towards stretching/compression factors of several thousand with low (<10%) overall losses in the future, affording promise for its application in high-power, multi-terawatt to petawatt laser systems.

Acknowledgements

This work is funded through the PFS grant of the Max-Planck Society. Financial support from the Extreme Light Infrastructure (ELI) and the DFG Cluster of Excellence (Munich Centre for Advanced Photonics) is also acknowledged. I. Ahmad thanks for his doctoral fellowship (HEC-DAAD 2006) from Higher Education Commission (HEC) of Pakistan in collaboration with German Academic Exchange Service (DAAD).

#117886 - $15.00 USD Received 28 Sep 2009; accepted 2 Oct 2009; published 8 Oct 2009
(C) 2009 OSA